Int. J. Heat Mass Transfer. Vol. 31, No. 2, pp. 349–358, 1988
Printed in Great Britain

0017–9310/88 $3.00 + 0.00

Fluidization and heat-transfer characteristics around a horizontal heated circular cylinder immersed in a gas fluidized bed

YASUO KUROSAKI
Department of Mechanical Engineering for Production, Tokyo Institute of Technology, Ohokayama, Meguro-ku, Tokyo 152, Japan

HIROSHI ISHIGURO
Institute of Engineering Mechanics, University of Tsukuba, Tennoudai, Sakura mura, Niihari-gun, Ibaraki-ken 305, Japan

and

KIYOSHI TAKAHASHI
Department of Mechanical Engineering for Production, Tokyo Institute of Technology, Ohokayama, Meguro-ku, Tokyo 152, Japan

(*Received* 2 *September* 1987)

Abstract—The fluidization and heat-transfer characteristics around a single horizontal heated circular cylinder immersed in a gas fluidized bed are fundamentally studied to clarify the mechanism of heat transfer in a fluidized-bed heat exchanger. The state of fluidization of particles is observed at various fluidization velocities. The fluctuating pressure and the local heat-transfer coefficient around the cylinder are measured. The local behavior of particles near the cylinder surface is classified into three categories. The correlation between the local heat-transfer characteristics and the state of the flows of particles and gas near the cylinder is obtained.

1. INTRODUCTION

IT IS IMPORTANT to study the heat-transfer augmentation in the heat exchanger for low-density energy such as waste heat for the effective use of thermal energy. Especially when the heat-transfer medium is a gas, the heat-transfer augmentation in the gas side makes a large contribution to the efficiency in the whole heat-transfer system. In the fluidized bed developed in chemical engineering, a large heat-transfer coefficient is given to the bed and the heat-transfer surface. Therefore, the fluidized bed is very effective as a high-performance heat exchanger for two media the temperature difference of which is small.

The heat-transfer characteristics around heated or cooled pipes immersed in a fluidized bed have been studied thus far. Particularly for a single horizontal heated circular cylinder, a fundamental component in a fluidized-bed heat exchanger, the mean heat-transfer coefficients were measured, and the empirical correlations were proposed [1–5]. The local heat-transfer coefficients around the cylinder were also measured [6–11], and the effects of fluidization velocity, cylinder diameter, particle size, particle properties, and system pressure on the heat-transfer coefficients were examined. From the point of view that the heat-transfer coefficients are strongly influenced by the behavior of particles and gas in the bed, their behavior was observed [12] and particle velocity was measured [10]. In consideration of the application to a fluidized-bed heat exchanger, the investigation of reduction of the pressure loss in the bed and distributor was carried out in several studies [13, 14].

However, the disagreement between experimental data and empirical correlations is large [5, 15]. It cannot be said that the generalized heat-transfer characteristics are studied on the basis of the mechanism of heat transfer. The reason is that the mechanism of heat transfer between a fluidized bed and heated or cooled pipes is very complicated because of the properties of particles, fluidizing gas and beds, and the behavior of particles and gas. Therefore, the usual method to correlate heat-transfer coefficients with influential parameters empirically is inadequate, and it is necessary to first grasp the phenomenon exactly.

In this study, the fluidization and heat transfer characteristics around a single horizontal heated circular cylinder immersed in a gas fluidized bed have been fundamentally examined to clarify the mechanism of heat transfer in a fluidized-bed heat exchanger. Importance was put on the clarification of the fluidization characteristics of particles and gas near

NOMENCLATURE

D	diameter of cylinder
Nu	Nusselt number, $\alpha D/\lambda$
P, p	instantaneous and fluctuating value of pressure on cylinder wall
ΔP	pressure loss in bed
Re	Reynolds number, UD/v
U	superficial gas velocity.

Greek symbols

α	heat-transfer coefficient
θ	degree from front stagnation point of cylinder
λ	thermal conductivity of gas
v	kinematic viscosity of gas.

Subscripts

m	mean value around cylinder
θ	local value around cylinder.

Superscript

$\bar{}$	time-averaged value.

the cylinder and in the bed as well as the heat transfer characteristics. The experiment was conducted at a low temperature to exclude the effect of radiation heat transfer. The state of fluidization of particles in the whole bed and near the cylinder was observed for various fluidization velocities covering fixed and fluidized beds. The fluctuating pressure and the local heat-transfer coefficient around the cylinder were also measured. Finally, the heat-transfer characteristics were discussed on the basis of the fluidization characteristics.

2. EXPERIMENTAL APPARATUS AND PROCEDURE

The schematic diagram of the experimental apparatus is shown in Fig. 1. A bed had a rectangular cross-section of 250 × 90 mm and a height of 1000 mm. The entire walls were made of acrylic plastic to permit visual observation. The distributor was a sandwich assembly of a 200 mesh metal screen, felt cloth and a perforated aluminum plate with an open area of 2.41%. A single circular cylinder 40 mm in diameter settled horizontally at a height 100 mm from the distributor. Glass beads of 400 μm average diameter sifted using 32 and 48 mesh metal screens were used in the experiment. These glass beads belong to Geldart's group B powder [16], which has the feature that the bubbles in the bed are comparatively large and tend to grow into bubble slugs. The bed was filled with the glass beads up to a 160 mm height from the bottom. A bell mouth-shaped section was attached at the outlet of the bed to prevent particles from flying out.

Four different types of circular cylinders schematically shown in Fig. 2 were provided to measure the fluidization and heat-transfer characteristics

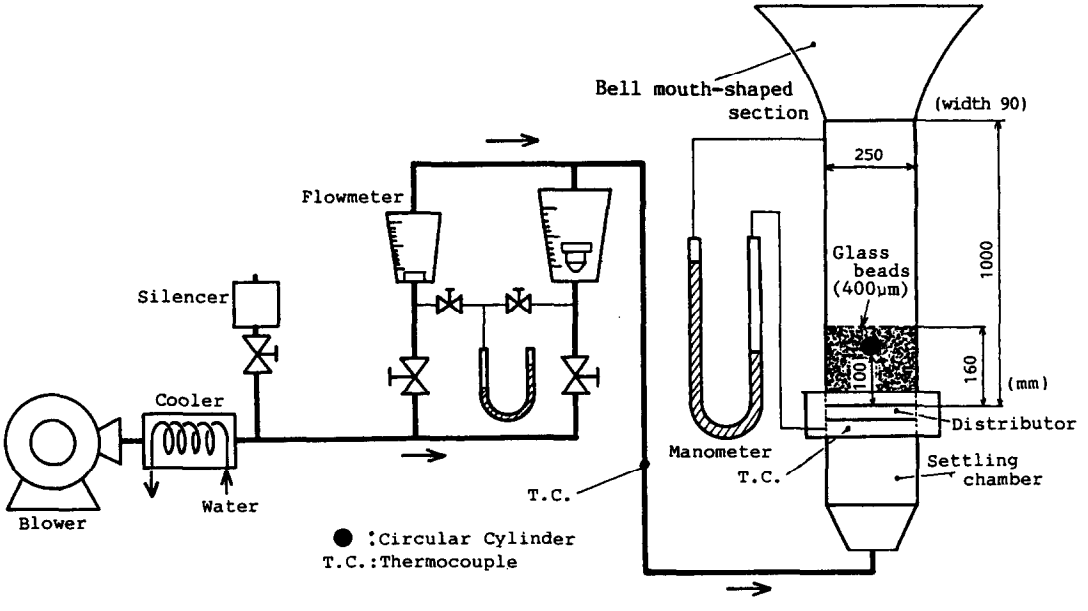

FIG. 1. Schematic diagram of the experimental apparatus.

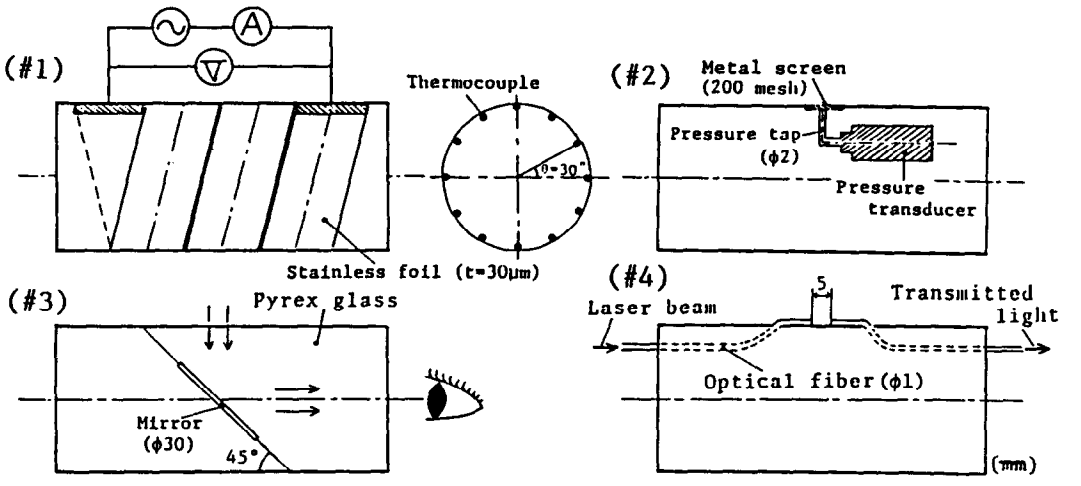

FIG. 2. Test cylinders.

around the cylinder. The bakelite cylinder (#1) 40 mm in diameter having a heater foil on the surface was manufactured to measure the local heat-transfer coefficient. A strip of stainless steel foil 30 μm thick, 20 mm wide and 420 mm long was bonded to the outer surface of the bakelite cylinder. This stainless steel foil served as a heater with the heat generated by passing alternating electric current through it. Twelve pairs of chromel–alumel thermocouples, each wire having a diameter of 0.1 mm, were placed in grooves directly beneath the foil at 30° intervals to measure the wall temperature. The cylinder was filled with a thermal insulator to avoid the heat loss from the inside of the cylinder and the test section was covered with a 50 mm thick thermal insulator. The temperature of the cylinder wall was controlled so that the difference between the mean temperature of the bed and the cylinder surface was about 10–20°C. Therefore, the effect of radiation heat transfer is negligible.

Pressure on the cylinder wall was measured by rotating a cylinder (#2) with a pressure transducer mounted in it around the cylinder axis. The pressure tap, 2 mm in diameter and about 10 mm in depth, was covered with a 200 mesh metal screen to prevent particles from coming into the tap. The pressure signal was amplified and processed using an analog signal processor.

The behavior of particles near the surface of a Pyrex glass cylinder (#3) was observed from the inside of the cylinder and was recorded by a videotape recorder. This glass cylinder was equipped with an interior mirror at an angle of 45° to its axis.

Another cylinder was constructed optically to examine the existence of particles and gas bubbles near the cylinder surface. Two pieces of optical fiber were fixed to the surface of the cylinder (#4) at an interval of 5 mm in the same line and parallel with the cylinder axis. The laser beam is able to pass through from one to the other optical fiber without particles intercepting the beam path. The transmitted laser beam was converted into an electrical signal by means of a photomultiplier tube. The existence of gas bubbles near the cylinder was determined by signal fluctuation.

The pressure drop in the bed was evaluated by subtracting the pressure drop due to the distributor measured without particles from the total pressure drop in both the bed and the distributor. The onset velocity of fluidization was determined by the relation between the superficial gas velocity and the pressure drop in the bed. The state of fluidization of particles in the whole bed was observed and was recorded by a videotape recorder through the transparent wall.

3. RESULTS AND DISCUSSION

3.1. *Flow characteristics*

3.1.1. *Pressure loss in the bed and minimum fluidizing velocity.* Figure 3 shows the pressure drop ΔP in the bed at various superficial gas velocities for both fixed and fluidized beds. In the fixed bed, ΔP for increasing U is a little larger than that for decreasing U; there is a small extent of hysteresis due to the initial filling structure as seen in Fig. 3. In the fluidized bed, ΔP is nearly constant and equal to the weight of particles per unit area in the bed shown by a dashed-dotted line. The minimum fluidizing velocity U_{mf} in the experiment was 0.135 m s^{-1}, which was determined by the intersection of the pressure drop vs velocity lines in the fully fluidized and fixed limits.

3.1.2. *Fluidization pattern in the whole bed.* The fluidization state in the whole bed has been found to depend upon the superficial gas velocity. Figure 4 shows the observed fluidization state in the bed for various superficial gas velocities. Thus far, there has been no reasonable characteristic length to define the Reynolds and Nusselt numbers on the fluidization and heat transfer around a horizontal heated circular cylinder immersed in a fluidized bed. Therefore, in

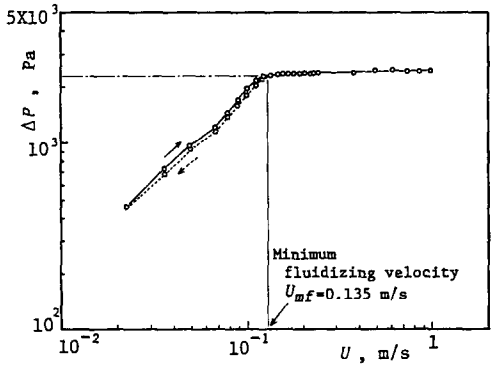

FIG. 3. Pressure loss in the bed.

this study, the diameter of the circular cylinder was adopted as the characteristic length of the Reynolds and Nusselt numbers.

The Reynolds number based on the minimum fluidizing velocity U_{mf} is equal to 345. The bed is not fluidized and is fixed in the range of $Re < 345$. But the state of the bed in this region was found to be classified into three categories according to the observation from the outside of the test section.

(1) Fixed state I. In the range of $Re < 240$, particles in the whole bed are still.

(2) Fixed state II. Though small size bubbles are sometimes generated near the side of the cylinder in the range of $240 < Re < 300$, they disappear before rising up to the surface of the particle bed.

(3) Fixed state III. In the range of $300 < Re < 345$, the bubbles generated around the cylinder reach the surface of the particle bed.

In the range of $Re > 345$, the bed exhibits good fluidization with the fluidized state being classified into three categories.

(1) Bubbling state. In the range of $345 < Re < 700$, bubbles begin to be generated from the distributor, and particles are mixed by the bubbles in the whole bed. With an increase of fluidization velocity, the generation of bubbles becomes more violent.

(2) Slugging state. In the range of $700 < Re < 1400$, bubbles from the distributor grow as large as the cross-section of the bed. It results in the fluctuations of the gas flow rate and the pressure in the bed.

(3) Turbulent state. In the range of $Re > 1400$, bubbles cannot be clearly observed, and particles and gas mix violently.

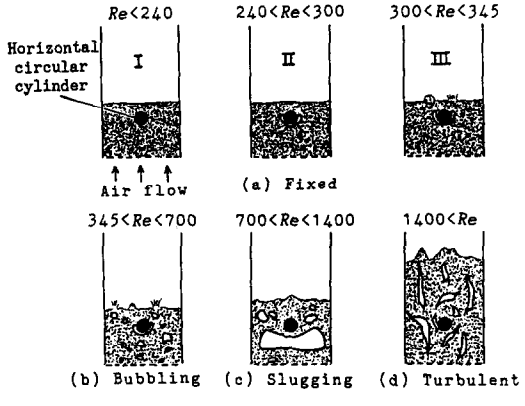

FIG. 4. Fluidization pattern in the whole bed.

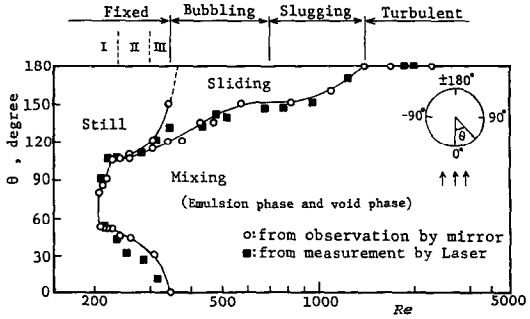

FIG. 5. Flow pattern of particles near the cylinder wall.

3.1.3. *Flow pattern of particles near the cylinder.* The state of the flow of particles and gas adjacent to the cylinder was observed by means of the Pyrex glass cylinder equipped with an interior mirror. As the particle movement on the cylinder surface was found to have bilateral symmetry around the circumference of the cylinder; therefore, only the results in the range of $0° \leqslant \theta \leqslant 180°$ are shown in Fig. 5. The state of fluidization in the whole bed is also indicated in the figure, where open circles denote the boundaries between the different regions of particle movement.

The local behavior of particles near the cylinder surface can be classified into three categories: (1) the still region where no particles move, (2) the sliding region where a group of particles slides on the surface of the cylinder and (3) the mixing region where the emulsion and void phases mix. The boundaries between these regions, especially between the sliding and mixing regions, fluctuate irregularly and lack uniformity in the axial direction of the cylinder. Therefore, the boundaries were decided as the temporal and spatial means primarily on the basis of the observation with a videotape recorder. Further explanations of these regions are given below.

(1) Still region. In the range of $Re < 200$, the still region occupies the whole circumference around the cylinder. With an increase of fluidization velocity, particles begin to move on the side wall of the cylinder. Then, the still region at the front and rear becomes narrow and disappears near the onset of fluidization.

(2) Sliding region. The sliding region exists between the mixing and still regions at the rear of the cylinder. The sliding region is considered to be formed due to the intermittent passage of bubbles with the flow of particles. Different kinds of sliding patterns could be observed according to the Reynolds number. For example at $Re = 340$ in the fixed bed, particles slide from the downstream side to the upstream side along the direction of the circumference. In the range

of $430 < Re < 700$, particles slide by oscillating from side to side. In the range of Re between the above two sliding patterns, there is an asymmetrical pattern in which a whole group of particles slides only in one direction. This is considered to be due to the bilateral asymmetrical passage of bubbles. Moreover, in the range of $700 < Re < 950$, particles come down and impinge the rear stagnation point intermittently; then they slide down to the upstream side symmetrically. In the range of $950 < Re < 1400$, the sliding direction of particles becomes random.

(3) Mixing region. At the incipient stage ($200 < Re < 240$) of movement of particles on the side wall of the cylinder, moving and still particles exist alternately in the direction of the axis of the cylinder. This local movement of particles near the cylinder surface could not be observed from the outside of the test section because the whole particle bed was apparently at rest. However, at a larger fluidization velocity in the fixed state, the region of moving particles spreads uniformly in the direction of the axis. In the range of $Re > 240$, the mixing region spreads to the front and rear of the cylinder; in the range of $Re > 1400$, the mixing region covers the whole circumference of the cylinder. The behavior of particles near the cylinder could not be clearly classified corresponding to the classification of the fluidization state in the whole bed into bubbling, slugging and turbulent states described previously; the mixing region was not subdivided.

Also in Fig. 5, the boundary of the mixing region determined by observing the fluctuation of the transmitted laser beam is shown by solid square symbols. The solid square symbols are in agreement with the result based on the observation using the Pyrex glass cylinder with a mirror. Therefore, the transmitted laser beam method adopted in this experiment was available to observe the state of particles and bubbles near the cylinder surface. It is considered that this local behavior of particles and gas near the cylinder surface has a great influence upon the local heat-transfer coefficient.

3.1.4. *Pressure signal on the cylinder wall.* Figure 6 shows the typical pressure signal on the cylinder wall at $\theta = 0°$, 90° and 180° in five different fluidization conditions in the whole bed. The fluctuating pressure patterns measured on the cylinder surface correspond to the behavior of bubbles and particles.

The still particles at the front and rear of the cylinder at $Re = 276$ in fixed state II give little fluctuating pressure at $\theta = 0°$ and 180°. But there is a small fluctuating pressure signal of about 15 Hz at $\theta = 90°$ due to the movement of particles on the side of the cylinder. At $Re = 340$ in fixed state III, the pressure has a low frequency fluctuation due to bubbles generated near the cylinder. As no bubbles are generated from the distributor in this state, the fluctuating pressure at $\theta = 0°$ is smaller than that at $\theta = 90°$.

At $Re = 560$ in the bubbling state, the fluctuating pressure around the whole circumference of the cylinder has a larger amplitude at low frequency due to bubbles from the distributor. In both the fixed and bubbling states, no bubbles pass by the position of $\theta = 180°$ on the cylinder surface; the movement of particles at the rear of the cylinder is not active. Therefore, the fluctuating pressure at $\theta = 180°$ is smaller than the ones at $\theta = 0°$ and 90°.

At $Re = 1010$ in the slugging state, there is periodic fluctuation of pressure with a signal frequency of about 2.5 Hz on the whole circumference. While a frequency of about 2.5 Hz is also observed locally around the circumference at larger fluidization velocity with large bubbles in the bubbling state, the frequency is considered to be determined due to the properties of the distributor, particles and bed and fluidization velocity. Moreover, at $Re = 3030$ in the turbulent state, the pressure has very random fluctuation with high frequency, and particles and gas mix violently.

3.1.5. *Distribution of intensity of pressure fluctuation on the cylinder wall.* Figure 7 shows the distribution of intensity $\sqrt{(\overline{p^2})}$ of pressure fluctuation on the cylinder wall for various fluidization velocities. In this figure, F, B, S and T denote the fixed, bubbling, slugging and turbulent states, respectively.

At $Re = 276$, 340 in the fixed state, the intensity of pressure fluctuation has a peak at $\theta = 90°$ due to movement of particles and generation of bubbles on the side of the cylinder. At $Re = 560$ in the bubbling state, the intensity has a peak at $\theta = 0°$ due to the impingement of bubbles upon the cylinder wall and decreases monotonously in the downstream direction. Figure 7 shows that the intensity of pressure fluctuation increases around the whole circumference with an increase of fluidization velocity from the bubbling state ($Re = 400, 560$) to the slugging state ($Re = 730, 1010$). It is caused by the fact that the cylinder surface area which bubbles reach spreads to the rear and the movement of particles becomes more violent with an increase of gas velocity.

Furthermore, at $Re = 2050, 3030$ in the turbulent state, particles and gas mix with each other violently and the whole bed becomes more homogeneous than that in the bubbling and slugging states. This results in a decrease of intensity of pressure fluctuation at $\theta = 0°$ and an increase of intensity at the rear of the cylinder due to the spread of the mixing region up to the rear stagnation point. Consequently, the distribution of the intensity of pressure fluctuation becomes flatter.

3.2. *Heat-transfer characteristics*

3.2.1. *Distribution of local heat-transfer coefficient.* Figure 8 shows the distribution of the local heat-transfer coefficient around the circumference of the cylinder for various fluidization velocities. The temperature at a 50 mm height from the distributor was used as the characteristic bed temperature which was almost uniform except near the cylinder. In this figure,

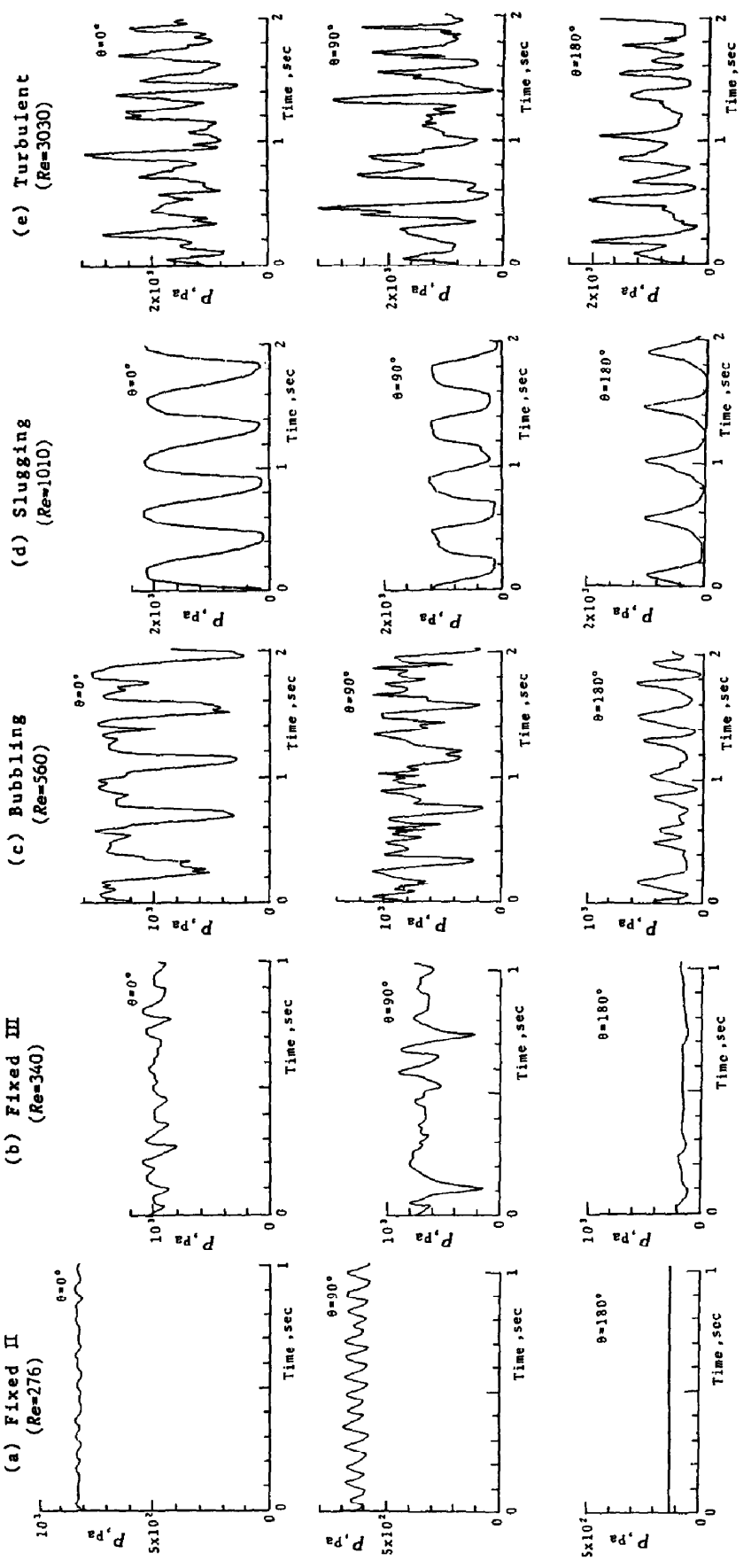

FIG. 6. Pressure signal on the cylinder wall.

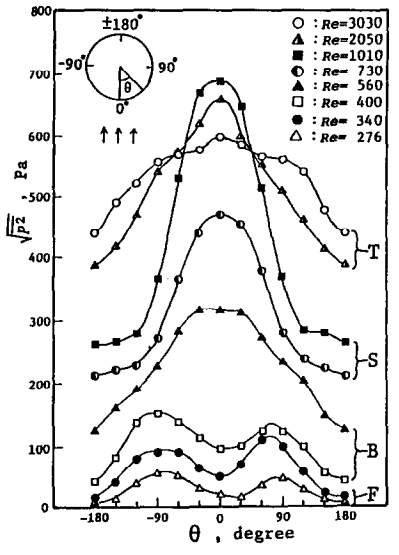

FIG. 7. Distribution of intensity of pressure fluctuations on the cylinder wall.

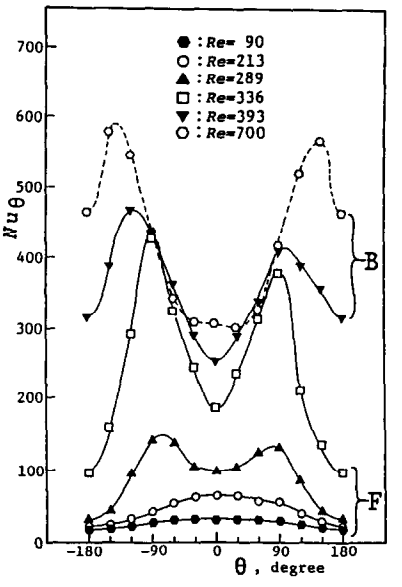

(a)

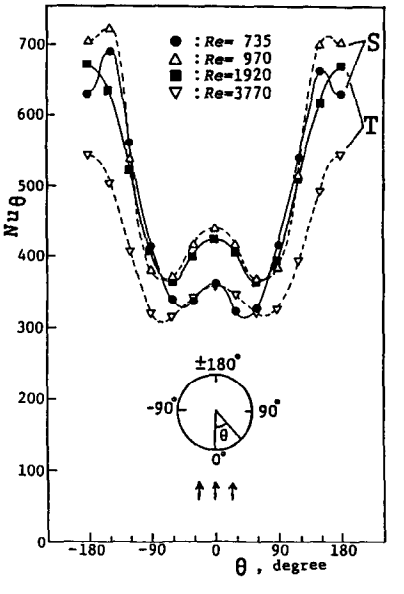

(b)

FIG. 8. Distribution of local heat-transfer coefficients: (a) case of low *Re*; (b) case of high *Re*.

F, B, S and T denote the fixed, bubbling, slugging and turbulent states, respectively.

At $Re = 90, 213$ in the fixed state I, Nu_θ has a maximum value at the front stagnation point of the cylinder; this was attributed to the effect of convective heat transfer of gas. With an increase of fluidization velocity (at $Re = 289$ in fixed state II and at $Re = 336$ in fixed state III), Nu_θ increases over the whole circumference. The beginning of movement of particles on the side wall of the cylinder causes the position of the maximum local heat-transfer coefficient to shift from the front stagnation point to the side wall due to the mixing effect of particles and gas.

As the fluidization state shifts to the bubbling state ($Re = 393, 700$) and to the slugging state ($Re = 735, 970$), the heat-transfer coefficient increases nearly around the whole circumference of the cylinder, and the increase at the rear of the cylinder is remarkable. The increase of the heat-transfer coefficient is attributed to the promotion of the mixing effect of particles near the cylinder. The bubbles generated in the distributor contribute to this mixing effect as seen in the observation of particles near the cylinder and the measurement of pressure fluctuation on the cylinder wall. The position of maximum Nu_θ moves toward the rear of the cylinder with an increase of fluidization velocity and reaches $\theta = 180°$ at $Re = 1920$.

As for Nu_θ at the front of the cylinder, Nu_θ is nearly constant in the range of $-30° < \theta < 30°$ at $Re = 700$. Nu_θ has a small peak at $\theta = 0°$ in the range of $Re > 700$, and the contour of distribution of Nu_θ hardly changes in the range of $Re \geqslant 735$. Moreover, at $Re = 3770$, Nu_θ decreases around the whole circumference of the cylinder. This is considered to be attributed to the decrease of density of particles in the bed because of the height increase of the fluidized bed although particles and gas mix randomly and violently in the turbulent state. As shown above, it is seen that the local behavior of particles and gas near the cylinder strongly effects the local heat transfer characteristics.

3.2.2. *Mean heat-transfer coefficient.* Figure 9 shows the mean heat-transfer coefficient vs the Reynolds number where the difference between the mean temperature on the wall of the cylinder and the characteristic one in the bed was used. Open triangles show Nu_m in the case of gas without particles and is larger by 30–40% than the result of McAdams [17] shown by a broken line, which is under the condition of

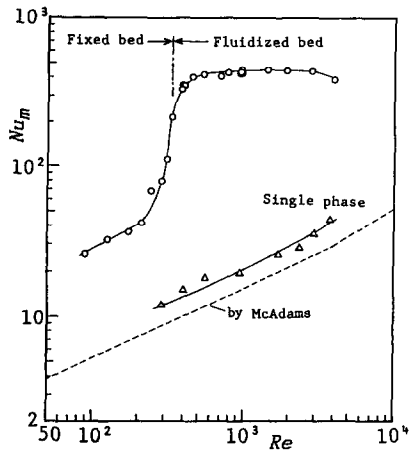

FIG. 9. Mean heat-transfer coefficient.

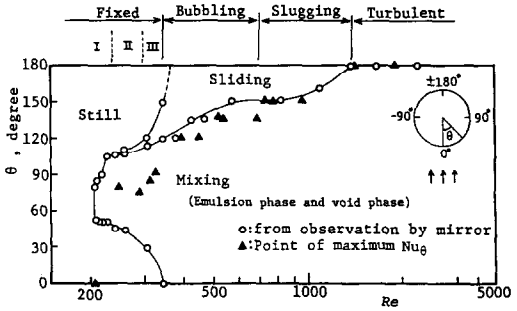

FIG. 10. Correlation between flow pattern of particles near the cylinder and position of maximum local heat-transfer coefficient.

constant wall temperature. This is considered to be mainly due to the effect of turbulence generated in the distributor. In the case with particles Nu_m, shown by open circles, begins to increase from about $Re = 250$, where bubbles are generated near the side of the cylinder in spite of the fixed bed. Although Nu_m in the fluidized bed also continues to increase, Nu_m approaches a constant value in the range of $700 < Re < 3000$. Accordingly, it was proved that the changes of state of fluidization in the whole bed and of the behavior of the particles near the cylinder in this range of Re have little influence on the mean heat-transfer coefficient. While Nu_m tends to decrease slightly in the range $Re > 3000$, Nu_m is about 10–20 times larger than that in the case of a single phase gas.

3.2.3. *Correlation between flow and local heat-transfer characteristics.* Figure 10 shows both the state of the flow of particles near the cylinder and the position of maximum local heat-transfer for various fluidization velocities. At nearly $Re = 200$ in fixed state I, the local heat-transfer coefficient becomes a maximum at the stagnation point ($\theta = 0°$) of gas flow. Moreover, in fixed states II and III, the maximum local heat-transfer coefficient takes place at nearly $\theta = 90°$, where particles and gas mix actively. As the state of fluidization of the bed shifts to the bubbling and slugging states, the position of the maximum local heat-transfer coefficient was found to be located near the boundary between the sliding and mixing regions, and to move toward the rear of the cylinder along with the boundary. In the turbulent state, the local heat-transfer coefficient becomes a maximum at $\theta = 180°$.

The reason why the boundary between the mixing and sliding regions have such a large heat transfer coefficient is described in the following. In this boundary region, renewal of particles with larger heat capacity than gas occurs more effectively than in the mixing and sliding regions. In the renewal of particles, hot particles near the cylinder are carried upward by the bubbles, and cold particles away from the cylinder are supplied into the space after the bubbles left, which was also observed by Noack [6]. In the mixing region, the density of particles is low although the movement of particles is active. In the sliding region, the movement of particles is weak although the density of particles is high. The behavior of particles in both the regions seems to correspond to less effective renewal of particles.

4. CONCLUSIONS

The fluidization and heat-transfer characteristics around a single heated circular cylinder immersed horizontally in a fluidized bed have been examined as the fundamental study about the mechanism of heat transfer in a fluidized-bed heat exchanger. Importance has been put on the clarification of the relation between the heat transfer and the fluidization characteristics of particles and gas near the cylinder and in the bed. The state of fluidization of particles has been observed for various fluidization velocities. Further, the fluctuating pressure and the local heat-transfer coefficient around the circumference of the cylinder have been measured. The heat-transfer characteristics have been discussed on the basis of the local fluidization characteristics. The conclusions are obtained as follows.

(a) The fluidization pattern of the whole bed shifts from the fixed state, to the bubbling, slugging and turbulent states with an increase of fluidization velocity. It is observed that particles move near the side wall of the cylinder and bubbles are also generated in some cases even in the fixed state.

(b) The local behavior of particles near the cylinder surface is classified into three categories: (1) the still region where no particles move, (2) the sliding region where a group of particles slides on the surface and (3) the mixing region where the emulsion phase and void phase mix. Furthermore, the changes in the three regions with an increase of fluidization velocity were clarified.

(c) The fluctuating pressure on the cylinder wall corresponds to the fluidization state in the bed and the local behavior of particles near the cylinder.

(d) The results of the local heat-transfer coefficient

vs the fluidization velocity clarify that in the fixed state the position of the maximum local heat-transfer coefficient shifts from the front stagnation point to the side of the cylinder nearly at the onset velocity of fluidization. In the fluidized state, the position moves toward the rear of the cylinder with an increase of fluidization velocity and the local heat-transfer coefficient increases remarkably at the rear of the cylinder.

(e) The high local heat-transfer coefficient is obtained at the boundary between the sliding and mixing regions.

A further study on the influence of the difference of the fluidization state due to the properties of particles upon the heat transfer in a fluidized bed was carried out, and the results will be given elsewhere.

In the future, the influence of the behavior of particles and gas near the cylinder on the heat-transfer characteristics should be clarified more quantitatively.

REFERENCES

1. H. A. Vreedenberg, Heat transfer between a fluidized bed and a horizontal tube, *Chem. Engng Sci.* **9,** 52–60 (1958).
2. N. I. Gel'perin, V. G. Ainshtein and F. D. Aronovich, The effect of screening on heat transfer in a fluidized bed, *Int. Chem. Engng* **3,** 185–190 (1963).
3. Y. Nagahashi and N. Hirayama, Heat transfer of a single horizontal tube in a fluidized bed, *Trans. Japan Soc. Mech. Engrs* **49,** 2163–2171 (1983), in Japanese.
4. S. Hukusako, N. Seki, S. Ishiguro and N. Eguchi, Heat transfer from horizontal immersed tube in particles bed, *Trans. Japan Soc. Mech. Engrs* **51,** 989–995 (1985), in Japanese.
5. N. S. Grewal and S. C. Saxena, Heat transfer between a horizontal tube and a gas–solid fluidized bed, *Int. J. Heat Mass Transfer* **23,** 1505–1519 (1980).
6. R. Noack, Lokaler Warmeubergang an Horizontalen Rohen in Wirbelschichten, *Chemie-Ingr-Tech.* **42,** 371–376 (1970).
7. B. V. Berg and A. P. Baskakov, Investigation of heat transfer between a fixed horizontal cylinder and a fluidized bed, *Int. Chem. Engng* **14,** 440–443 (1974).
8. N. I. Gel'perin, V. G. Ainshtein and A. V. Zaikovskii, Variation of heat-transfer intensity around the perimeter of a horizontal tube in a fluidized bed, *J. Engng Phys.* **10,** 473–475 (1966).
9. R. Chandran, J. C. Chen and F. W. Staub, Local heat-transfer coefficients around horizontal tubes in fluidized beds, *Trans. Am. Soc. Mech. Engrs*, Series C, *J. Heat Transfer* **102,** 152–157 (1980).
10. M. Iwashko, D. Mosiemian, M. M. Chen and B. T. Chao, Effect of solid particle velocity distribution on local heat-transfer coefficients in fluidized beds, *Proceedings of 23rd National Heat Transfer Conference*, Denver, Colorado, HTD-Vol. 46, pp. 61–67 (August 1985).
11. N. Seki, S. Fukusako, K. Torikoshi and J. Tanaka, Local heat transfer on a horizontal tube immersed in a fluidized bed, *Trans. Japan Soc. Mech. Engrs* **48,** 1985–1993 (1982), in Japanese.
12. D. H. Glass and D. Horrison, Flow patterns near a solid obstacle in a fluidized bed, *Chem. Engng Sci.* **19,** 1001–1002 (1964).
13. T. Aihara, S. Maruyama, S. Aya and M. Hongoh, Heat-transfer characteristics of a low-pressure-loss fluidized-bed heat exchanger with single-row tubes, *Trans. Japan Soc. Mech. Engrs* **52,** 1718–1725 (1986), in Japanese.
14. M. Kumada, K. Ogawa, Y. Watanabe and I. Mabuchi, Basic study on a fluidized-bed heat exchanger (1st Report), *Trans. Japan Soc. Mech. Engrs* **53,** 1024–1031 (1987), in Japanese.
15. J. C. Chen, Heat transfer to submerged tubes in fluidized beds. In *Two-phase Flow and Heat Transfer, China–U.S. Progress* (Edited by X. J. Chen and T. N. Veziroğlu), pp. 505–520. Hemisphere, Washington, DC (1984).
16. D. Geldart, Types of gas fluidization, *Powder Technol.* **7,** 285–292 (1973).
17. W. H. McAdams, *Heat Transmission*, 3rd Edn, p. 259. McGraw-Hill, New York (1954).

CARACTERISTIQUES DE FLUIDISATION ET DE TRANSFERT THERMIQUE AUTOUR D'UN CYLINDRE CIRCULAIRE HORIZONTAL CHAUD ET IMMERGE DANS UN LIT FLUIDISE GAZEUX

Résumé—La fluidisation et le transfert thermique autour d'un unique cylindre circulaire horizontal chauffé et immergé dans un lit fluidisé gazeux sont étudiés pour clarifier le mécanisme du transfert de chaleur dans un échangeur thermique à lit fluidisé. L'état de la fluidisation des particules est observé à différentes vitesses de fluidisation. On mesure la pression fluctuante et le coefficient local de transfert thermique autour du cylindre. Le comportement local des particules près de la surface du cylindre est classé en trois catégories. On obtient la corrélation entre les caractéristiques locales du transfert et l'état de l'écoulement des particules et du gaz près du cylindre.

FLUIDISIERUNG UND WÄRMEÜBERTRAGUNG IN DER UMGEBUNG EINES HORIZONTALEN BEHEIZTEN KREISZYLINDERS IN EINEM FLIESSBETT

Zusammenfassung—Fluidisierung und Wärmeübergang in der Umgebung eines einzelnen horizontalen beheizten Kreiszylinders, der sich in einem Gas-Fließbett befindet, wurde grundsätzlich untersucht, um den Mechanismus der Wärmeübertragung in einem Wirbelschicht-Wärmeaustauscher zu klären. Der Fluidisierungszustand wird bei unterschiedlichen Geschwindigkeiten beobachtet. Der schwankende Druck und der lokale Wärmeübergangskoeffizient um den Zylinder werden gemessen. Das lokale Verhalten von Partikeln an der Zylinderoberfläche wird in drei Kategorien eingeteilt. Man erhält eine Korrelation zwischen dem lokalen Wärmeübergang und dem Strömungszustand von Partikeln und Gas am Zylinder.

ХАРАКТЕРИСТИКИ ПСЕВДООЖИЖЕНИЯ И ТЕПЛОПЕРЕНОСА У ГОРИЗОНТАЛЬНОГО НАГРЕВАЕМОГО ЦИЛИНДРА, ПОГРУЖЕННОГО В ПСЕВДООЖИЖЕННЫЙ ГАЗОМ СЛОЙ

Аннотация—Характеристики псевдоожижения и теплопереноса у единичного горизонтального цилиндра, погруженного в псевдоожиженный газом слой, изучаются для выяснения механизма теплопереноса в теплообменнике с псевдоожиженным слоем. Состояние псевдоожижения частиц наблюдалось при различных скоростях фильтрации газа. Измерены флуктуации давления и локальные коэффициенты теплообмена у цилиндра. Локальное поведение частиц у поверхности цилиндра классифицировано по трем категориям. Получена корреляция между интенсивностью локального теплопереноса и характеристиками частиц и газа у цилиндра.